Journal Pre-proofs

Potent, non-covalent reversible BTK inhibitors with 8-amino-imidazo[1,5-*a*]pyrazine core featuring 3-position bicyclic ring substitutes

Jian Liu, Deodial Guiadeen, Arto Krikorian, Xiaolei Gao, James Wang, Sobhana Babu Boga, Abdul-Basit Alhassan, Wensheng Yu, Oleg Selyutin, Younong Yu, Rajan Anand, Jiayi Xu, Joseph Kelly, Joseph L. Duffy, Shilan Liu, Chundao Yang, Hao Wu, Jiaqiang Cai, Chad Bennett, Kevin M. Maloney, Sriram Tyagarajan, Ying-Duo Gao, Thierry O. Fischmann, Jeremy Presland, My Mansueto, Zangwei Xu, Erica Leccese, Jie Zhang-Hoover, Ian Knemeyer, Charles G. Garlisi, Peter Stivers, Philip E. Brandish, Alexandra Hicks, Ronald Kim, Joseph A. Kozlowski

PII: S0960-894X(20)30501-1
DOI: https://doi.org/10.1016/j.bmcl.2020.127390
Reference: BMCL 127390

To appear in: *Bioorganic & Medicinal Chemistry Letters*

Received Date: 8 May 2020
Revised Date: 1 July 2020
Accepted Date: 3 July 2020

Please cite this article as: Liu, J., Guiadeen, D., Krikorian, A., Gao, X., Wang, J., Babu Boga, S., Alhassan, A-B., Yu, W., Selyutin, O., Yu, Y., Anand, R., Xu, J., Kelly, J., Duffy, J.L., Liu, S., Yang, C., Wu, H., Cai, J., Bennett, C., Maloney, K.M., Tyagarajan, S., Gao, Y-D., Fischmann, T.O., Presland, J., Mansueto, M., Xu, Z., Leccese, E., Zhang-Hoover, J., Knemeyer, I., Garlisi, C.G., Stivers, P., Brandish, P.E., Hicks, A., Kim, R., Kozlowski, J.A., Potent, non-covalent reversible BTK inhibitors with 8-amino-imidazo[1,5-*a*]pyrazine core featuring 3-position bicyclic ring substitutes, *Bioorganic & Medicinal Chemistry Letters* (2020), doi: https://doi.org/10.1016/j.bmcl.2020.127390

Graphical Abstract

To create your abstract, type over the instructions in the template box below.
Fonts or abstract dimensions should not be changed or altered.

Potent, non-covalent reversible BTK inhibitors with 8-amino-imidazo[1,5-*a*]pyrazine core featuring 3-position bicyclic ring substitutes

Jian Liu and et al.

Leave this area blank for abstract info.

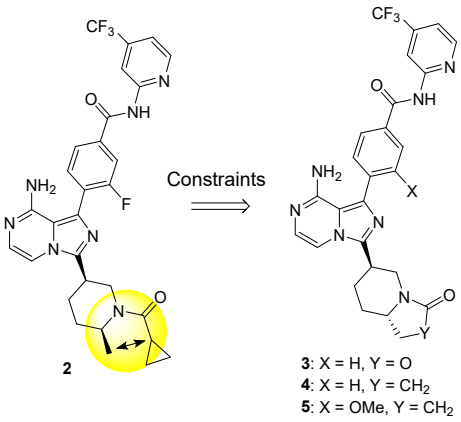

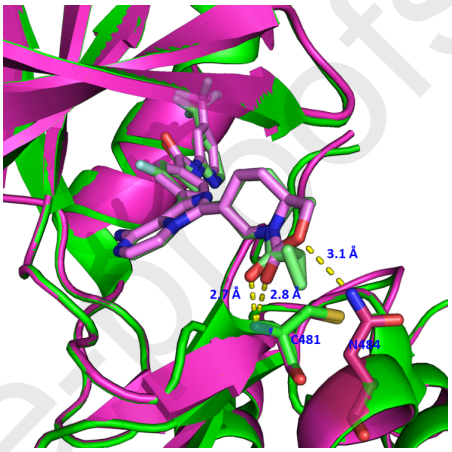

ELSEVIER

Bioorganic & Medicinal Chemistry Letters
journal homepage: www.elsevier.com

Potent, non-covalent reversible BTK inhibitors with 8-amino-imidazo[1,5-*a*]pyrazine core featuring 3-position bicyclic ring substitutes

Jian Liu[a]*, Deodial Guiadeen[a], Arto Krikorian[a], Xiaolei Gao[a], James Wang[a], Sobhana Babu Boga[a], Abdul-Basit Alhassan[a], Wensheng Yu[a], Oleg Selyutin[a], Younong Yu[a], Rajan Anand[a], Jiayi Xu[a], Joseph Kelly[a], Joseph L. Duffy[a], Shilan Liu[b], Chundao Yang[b], Hao Wu[b], Jiaqiang Cai[b], Chad Bennett[a], Kevin M. Maloney[a], Sriram Tyagarajan[a], Ying-Duo Gao[a], Thierry O. Fischmann[a], Jeremy Presland[a], My Mansueto[a], Zangwei Xu[a], Erica Leccese[a], Jie Zhang-Hoover[a], Ian Knemeyer[a], Charles G. Garlisi[a], Peter Stivers[a], Philip E. Brandish[a], Alexandra Hicks[a], Ronald Kim[a], Joseph A. Kozlowski[a]

[a] *Department of Early Development and Discovery Sciences, Merck & Co., Inc., 2000 Galloping Hill Road, Kenilworth, NJ 07033, USA*
[b] *WuXi AppTec Co. Ltd, 288 FuTe Zhong Road, No. 1 Building, WaiGaoQiao Free Trade Zone, Shanghai 200131, PR China*

ARTICLE INFO

Article history:
Received
Revised
Accepted
Available online

Keywords:
Bruton's Tyrosine Kinase
Structure based drug design
Kinase selectivity
Rat CIA model
X-ray crystal structure

ABSTRACT

Bruton's tyrosine kinase (BTK) is a Tec family kinase with a well-defined role in the B cell receptor (BCR) pathway. It has become an attractive kinase target for selective B cell inhibition, and for the treatment of B cell related diseases. Many BTK inhibitors have been discovered for the treatment of cancer and rheumatoid arthritis, including a series of BTK inhibitors based on 8-amino-imidazo[1,5-*a*]pyrazine we recently reported. The X-ray crystal structures of BTK with inhibitors were also published, which provided great help for the SAR design. Here we report our SAR work introducing ring constraints for the 3-position piperidine amides on the BTK inhibitors based on 8-amino-imidazo[1,5-*a*]pyrazine. This modification improved the potency in BTK inhibitions, as well as the PK profile and the off-target selectivity. The dose-dependent efficacy of two BTK inhibitors was observed in the rat collagen induced arthritis (CIA) model.

Bruton's tyrosine kinase (BTK) is a Tec family kinase expressed in certain immune cells including B cells, mast cells and macrophages.[1,2] It plays a critical role in multiple pathways such as the B cell receptor (BCR) and Fcγ receptor (FcR) signaling cascades, where it regulates the survival, activation, proliferation, differentiation and maturation of B cells.[3,4] The role of BTK in these pathways makes the enzyme a uniquely attractive target for the treatment of B cell related diseases. BTK selective inhibitors can be used as cancer therapies and for the treatment of rheumatoid arthritis (RA).[5] Currently the three approved BTK inhibitor drugs are ibrutinib,[6] acalabrutinib,[7] and zanubrutinib[8] (Figure 1). Many BTK inhibitors are in clinical trials.[9] These approved drugs are irreversible covalent binding inhibitors. The covalent binding BTK inhibitor ibrutinib was approved for the treatment of mantle cell lymphoma and chronic lymphocytic leukemia. However, a small portion (5.3%) of the patients on ibrutinib therapy encountered relapse for chronic lymphocytic leukemia. This relapse was primarily caused by a cysteine to serine mutation at C481, which is the covalent binding residue. Thus, the mutation results in significant loss in binding affinity of ibrutinib to mutant BTK.[10] A potent non-covalent BTK inhibitor, which does not utilize C481 covalent binding for affinity, could still be efficacious for patients with this mutation. Several research groups have reported various non-covalent binding BTK inhibitors,[11,12] including our previously published BTK inhibitors based on 8-

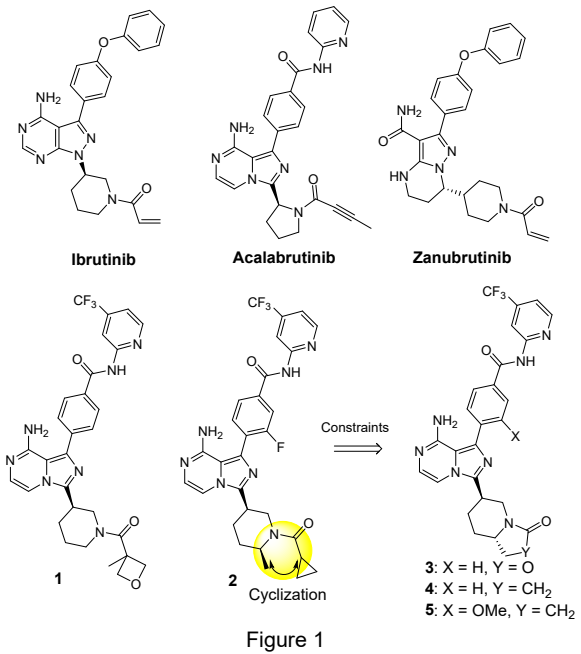

Figure 1

ami[illegible]-yl) and **2** (Figure 1).[13,14,15] Ibrutinib showed excellent efficacy in the rat collagen induced arthritis model (CIA), indicating its potential use for the treatment of RA.[16] Our previously reported non-covalent BTK inhibitor **2** also demonstrated dose-dependent efficacy in the rat CIA model.

We also reported the X-ray crystal structure of compound **2** in the binding pocket of BTK.[13] The cyclopropylamide substituent on the 3-piperidine has a trans conformation forced by the methyl group with the carbonyl oxygen forming a hydrogen bond with the C481 NH. The alpha carbon of the amide is in the position that can be cyclized to the piperidine 2-carbon to fix the amide carbonyl in the proper orientation for the hydrogen binding with C481 backbone NH. Thus, we designed compounds **3** (Y = O) and **4** (Y = CH_2) with a cyclic carbamate or lactam ring constraint. We modeled that the ring constraints would fix the carbonyl oxygen in the direction to hydrogen bonding with C481 backbone NH, which potentially could increase the binding potency while also improving the PK profile.

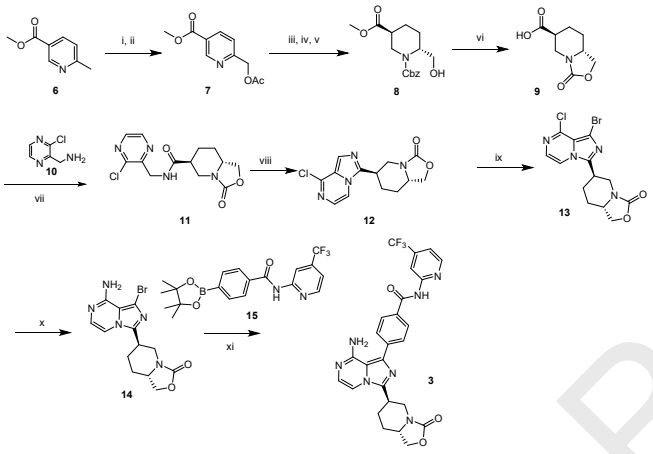

Scheme 1. i. mCPBA, CH_2Cl_2, rt; ii. Ac_2O, 130 °C, 1h, 35% two steps; iii. $NaBH_3CN$, AcOH, rt; 24 h; iv. Cbz-Cl (2eq), $NaHCO_3$, 0 °C to rt, 24 h, 34% two steps; v. HCl, MeOH, reflux, 24 h, 55%; vi. LiOH, THF/H_2O, rt, 24 h, 100%; vii. ^{i}PrOCOCl (1eq), TEA (2eq), 3 h, 73%; viii. $POCl_3$, CH_3CN, rt, 15 h, 94%; ix. NBS, DMF, rt, 1 h, 83%; x. NH_3/^{i}PrOH, 100 °C, 7 h, sealed tube, 74%; xi. Pd(dppf)Cl_2, K_2CO_3, dioxane, 100 °C, 2 h, 36%.

The preparation of **3** is depicted in Scheme 1, with all reaction reagents and conditions noted.[17] The synthesis started from methyl 6-methylnicotinate **6**, which was treated with mCPBA for the formation of pyridine N-oxide. The N-oxide was then reacted with acetic anhydride to the N-oxide acetate, followed by a rearrangement reaction to produce methyl 6-(acetoxymethyl) nicotinate **7**. The pyridine ring in **7** was then reduced to the piperidine by sodium cyano borohydride. The formed piperidine nitrogen was protected by reacting with benzyl chloroformate. Later the acetate was hydrolyzed by lithium hydroxide in THF/water to provide trans (+/-) 1-benzyl 3-methyl-6-(hydroxymethyl)piperidine-1,3-dicarboxylate **8**. The racemate **8** was resolved by chiral HPLC to provide 1-benzyl 3-methyl (3S,6R)-6-(hydroxymethyl)piperidine-1,3-dicarboxylate **8**. The cyclic carbamate was formed along with the hydrolysis of the methyl ester when **8** was treated with lithium hydroxide in mixed solvent of tetrahydrofuran and water at room temperature overnight to generate compound **9** (6S,8*a*R)-3-oxohexahydro-3H-oxazolo[3,4-a]pyridine-6-carboxylic acid. Acid **9** was then coupled with (3-chloropyrazin-2-yl)methanamine **10** after being activated by isopropyl chloroformate to form (6S,8*a*R)-N-((3-chloropyrazin-2-yl)methyl)-3-oxohexahydro-3H-oxazolo[3,4-a]pyridine-6-carboxamide **11**. The amide **11** was subsequently hexahydro-3H-oxazolo[3,4-a]pyridin-3-one **12** after being treated with phosphoryl trichloride in acetonitrile with a quantitative yield. Bromation of **12** using NBS in DMF provided an excellent yield of bromo compound **13**. The 8-chloro substituent in compound **13** was then converted to 8-amino by treatment with ammonium hydroxide in isopropanol in a sealed reaction vessel at 100 °C for 7 hours to give a moderate yield of **14**. Suzuki coupling of **14** with boronic ester **15**[13] afforded the final compound **3**.

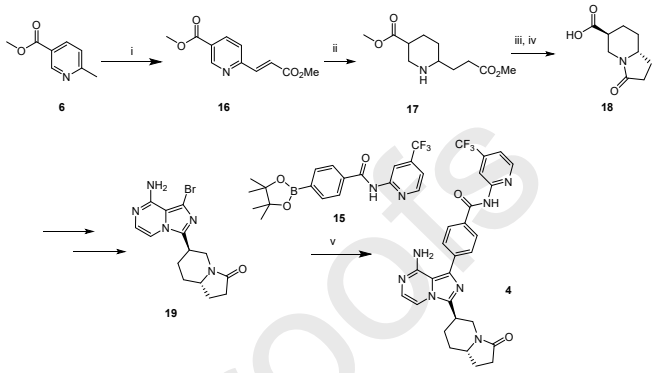

Scheme 2. i. Ethyl 2-oxoacetate, Ac_2O, 130 °C, 48 h, 73%; ii. Pd(OH)$_2$/C, AcOH, H_2 (40 psi), 18 h; iii. TEA, MeOH, rt, 18 h; iv. NaOMe (2 eq), MeOH, 50 °C, HCl, 76% three steps; v. Pd(dppf)Cl_2, K_2CO_3, dioxane, 100 °C, 2 h, 36%.

We then synthesized the bicyclic lactam acid **18**, which could be converted to the final target **4**. The preparation of **4** (X = CH_2) with an alternative lactam ring constraint started with the same starting material methyl 6-methylnicotinate **6** (Scheme 2). It was heated together with ethyl 2-oxoacetate in acetic anhydride at 130 °C for two days to afford **16** with good yield. Hydrogenation was carried out in acetic acid catalyzed by palladium hydroxide on carbon under 40 psi hydrogen atmosphere overnight to generate the fully reduced piperidine compound **17**. The lactam was formed as a cis/trans mixture when **17** was stirred in methanol along with triethylamine at room temperature for 18 hours. The lactam was then treated with sodium methoxide in methanol at 50 °C to hydrolyze the ester to acid, and at the same time the cis/trans mixture of acid isomerized to the thermodynamically more stable trans acid **18**. The acid **18** was precipitated as a racemate in water as white solid when treated with hydrochloric acid. Following the same chemistry described in Scheme 1 for the preparation of **14**, acid **18** was converted to the intermediate **19** as a racemate which was resolved to two enantiomers. The desired (6R,8*a*S) enantiomer **19** was coupled with **15** to form the final product **4** by a Suzuki coupling reaction.[17]

Table 1. In vitro BTK inhibition data for **2**, **3** and **4**

Compound	BTK Enzymatic Assay[a] IC_{50} (nM)	hPBMC Assay[a] IC_{50} (nM)	Human whole Blood[a] IC_{50} (nM)
2	0.31	4.0	94
3	0.083	5.8	36
4	0.1	2.5	24

a. Reported values are the average of ≥ 2 independent measurements with standard deviation less than 3-fold of the reported mean

evaluated in the BTK enzymatic binding assay, the hPBMC B cell functional assay and the human whole blood B cell functional assay.[13] The data are summarized in Table 1. Compared to **2**, both the cyclized **3** and **4** with carbamate and lactam as the bicyclic constraints showed improved binding potency to BTK enzyme by more than 3-fold. Furthermore, the cellular and whole blood activities were also significantly improved. The enantiomer of compound **4** is 150-fold less potent.

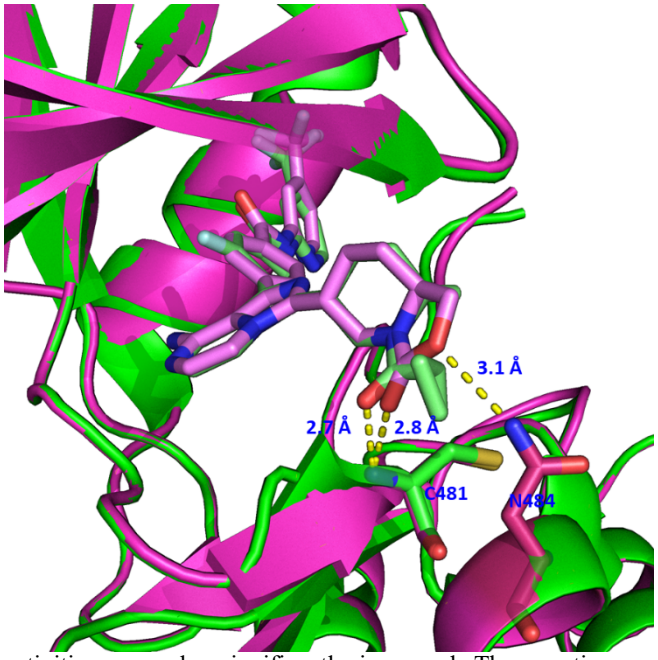

Figure 2. Overlay of X-ray crystal structures of compound **2** (green) and **3** (purple) binding to BTK enzymes.

We were able to get the X-ray co-crystal structure of **3** bound to the BTK enzyme. Figure 2 shows the overlay of the crystal structures of both **2** and **3** binding to the BTK enzyme. The carbamate derivative **3** has the similar binding mode to **2** in the back pocket, and the hinge region as described in the previous publication.[13] These interactions provide the high binding potency and the selectivity. The carbonyl of the carbamate in the bicyclic ring in **3** (purple) is locked in the conformation to form a hydrogen bond with the amide NH of C481. In the meantime, the carbamate oxygen forms a hydrogen bond with the side chain amide of N484, which provides the extra binding potency for **3** compared to **2**.

The carbamate functional group is potentially a soft spot for metabolism, specially at the carbon connected to the carbamate oxygen. To block the potential metabolism, we prepared compounds with methyl or gem-dimethyl substitution (Scheme 3). The alcohol **8** was oxidized to the aldehyde using Dess-Martin reagent in methylene chloride at room temperature, followed by addition of the methyl magnesium bromide in THF at -78 °C to provide the alcohol compound **20** in a moderate yield (50%). Cyclization occurred when **20** was stirred under a basic condition in the mixture of tetrahydrofuran/water and lithium hydroxide to form the cyclic carbamate **21** with a good yield as a mixture of two diastereomers. In the same sequence, the secondary alcohol **20** could be oxidized again by Dess-Martin reagent to a ketone, followed by addition of the methyl magnesium bromide to provide the tertiary alcohol **22**. When **22** was treated with lithium hydroxide in tetrahydrofuran/water, the cyclic carbamate bicyclic carboxylic acid **23** with the gem-dimethyl formed in a good yield (79%). Bicyclic acids **21** and **23** were converted to the final compound **24A**, **24B** and **25**, applying the similar chemistry in Scheme 1.[17]

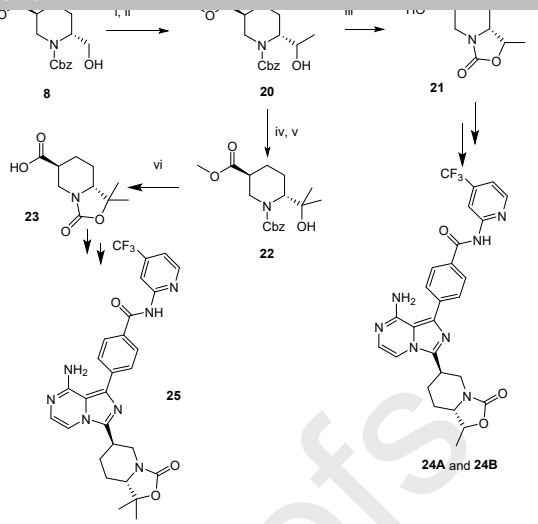

Scheme 3. i. Dess-Martin, CH_2Cl_2, rt, 85%; ii. MeMgBr, THF, -78 °C, 50%; iii. LiOH (2eq), THF/H_2O, rt, 12 h, 75%; iv. Dess-Martin, CH_2Cl_2, rt, 60%; v. MeMgBr, THF, -78 to -25 °C, 4 h, 33%; vi. LiOH (2eq), THF/H_2O, 3 h, 79%.

Table 2. SAR data of 3-position bicyclic substitutes

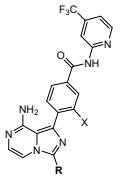

Compound # R, X	Enzymatic Assay[a] IC_{50} (nM)	hPBMC Assay[a] IC_{50} (nM)	Human whole Blood EC_{50} (nM)
24A X = H	0.13	4.9	86
24B X =H	0.11	3.2	63
25 X = H	0.12	2.8	58
26 X = H	0.26	7.2	263
27 X = H	25	582	NT
28 X = H	7.2	403	NT
29 X = H	0.67	39	204
30 X = F	1.7	39	NT
31 X =F	0.1	5.8	78
32 X =H	0.26	16	104

a. I

standard deviation less than 3-fold of the reported mean
NT = Not Tested

To explore other constrained bicyclic substitutes on the 3-position of the core imidazo[1,5-a]pyrazine, a series of bicyclic analogs were prepared (Table 2). The precursor bicyclic acids were synthesized and then the same chemistry in Scheme 1 was applied to generate the final target molecules in the table.[17] This series of compounds with 8-amino-imidazo[1,5-a]pyrazine core and various selected 3-position bicyclic ring substitutes were evaluated in the BTK enzymatic, cellular and whole blood assays. The BTK enzyme tolerated many changes with these bicyclic ring substitutes on the 3-position. Compound **24a**, **24b** and **25** with methyl substitutes on the carbon alpha to the carbamate oxygen were tolerated with similar activity to **3** in enzymatic, cellular and whole blood assays. This series of compounds maintained most of the BTK inhibition potency for compounds **26** with morpholinyl bicyclic lactam, **29** with octohydroindolinzinyl, **30** with octohydro-*4H*-quinolizinonyl, **31** with hexahydropyrido[2,1-c][1,4]oxazin-4(3H)-onyl, and **32** with 2-methyloctahydro-4H-pyrido[1,2-a]pyrazin-4-onyl. However, compound **27** with the bicyclic morpholine carbamate and **28** with the bicyclic methyl urea are much less potent, which may have been caused by unfavored interactions with the BTK enzyme.

Previously, we demonstrated the SAR of substitutes on the middle phenyl that variable substitution X at the 3-position is tolerated by BTK enzyme for other reported series of BTK inhibitors based on 8-amino-imidazo[1,5-*a*]pyrazine core.[13,14,15] Thus we further explored this SAR on the impact of BTK inhibition activity with different substitutes on this position based on compound **4**. These compounds can be prepared by applying boronic esters like **15** in Scheme 1 with different substitutes on the phenyl ring 3-position.[17] The compounds were evaluated in the BTK enzymatic, cellular and whole blood assays and the data are shown in Table 3. There is limited space around the middle phenyl to allow only small substitutes (X) on the phenyl 3-position, such as OMe (**5**), F (**33**), OEt (**34**), OCF_2H (**35**), OH (**36**), and O^{c}Pr (**37**), all of which maintain the BTK enzymatic inhibition with sub-nanomolar potency. However, there is significantly 20-fold loss of potency when the substitution was changed from cyclopropyl to a slightly bigger isopropyl (**38**). The bigger size substitution like phenoxy (**39**) resulted in further loss of potency. The polar and electron-withdrawing substitutes exemplified by carbamide (**40**), carboxylic acid (**41**), cyano (**42**), CF_2CH_3 (**43**), CF_3 (**44**) and OCF_3 (**45**) all caused significant loss of the activity in enzymatic and cellular assays.

Most of the potent BTK inhibitors were screened through a small kinome panel with representative kinases from the Tec and Src family to evaluate the selectivity of this series BTK inhibitors over other kinases. The data for compound **3**, **4**, **5**, **25** and **37** are listed in Table 5 with the IC_{50} and fold of selectivity over BTK enzyme. All these BTK inhibitors demonstrated high selectivities over other Tec and Src family kinases. Comparing the cyclocarbamate **3** to the lactam **4**, compound **3** has better selectivity (fold) across most kinases in the panel. This improved selectivity can be rationalized by the hydrogen bond interaction of the carbamate oxygen with N484 side chain amide described in the X-ray crystal structure above. This interaction does not exist with the lactam structure of **4**. When the gem-dimethyl was introduced on the carbon next to the oxygen in the carbamate, compound **25** showed lower selectivities compared to **3**. The methoxy and cyclopropoxy substitutes on the phenyl 3-position have significant impact on the BTK selectivity, with an increased selectivity

d **5** showed better selectivity than **4**, while **37** had better selectivity than **5**.

Table 3: SAR data for phenyl 3-substitutes

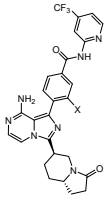

Compound #	X	BTK Enzymatic Assay[a] IC_{50} (nM)	hPBMC Assay[a] IC_{50} (nM)	Human whole Blood EC_{50} (nM)
4	H	0.1	2.5	24
5	OMe	0.21	17	30
33	F	0.11	4.0	101
34	OEt	0.16	10	92
35	OCF_2H	0.48	20	415
36	OH	0.58	11	NT
37	O^{c}Pr	0.58	12	494
38	O^{i}Pr	5.7	41	NT
39	OPh	11	310	NT
40	$CONH_2$	348	>3000	NT
41	COOH	83	1410	NT
42	CN	6.3	267	NT
43	CF_2CH_3	831	822	NT
44	CF_3	>1000	>3000	NT
45	OCF_3	10	74	NT

b. Reported values are the average of ≥2 independent measurements with standard deviation less than 3-fold of the reported mean
NT = Not Tested

Table 4: Selectivity of compound **3**, **4, 5, 25** and **37** over Tec and Src family kinases

Kinase	Comp **3** IC_{50} (nM) (fold x)	Comp **4** IC_{50} (nM) (fold x)	Comp **5** IC_{50} (nM) (fold x)	Comp **25** IC_{50} (nM) (fold x)	Comp **37** IC_{50} (nM) (fold x)
BTK	0.083	0.1	0.21	0.12	0.58
BLK	22 (265)	8.3 (83)	101 (480)	17 (140)	309 (532)
BMX	13 (157)	11 (110)	19 (90)	5.6 (47)	64 (110)
CSK	290 (3500)	162 (1620)	227 (1080)	350 (2900)	717 (1236)
ERBB4	34 (410)	24 (240)	160 ((762)	23 (190)	3300 (5700)
FGR	26 (313)	NT	64 (304)	34 (283)	263 (453)
FRK	46 (554)	34 (340)	154 (733)	36 (300)	530 (913)
FYN	18 (219)	87 (870)	1230 (5900)	212 (1700)	7400 (12758)
LCK	11 (132)	5.9 (59)	26 (124)	13 (110)	182 (313)
LYNB	49 (590)	20 (200)	162 (771)	79 (660)	865 (1500)
PTK6	50 (600)	42 (420)	84 (400)	24 (200)	320 (550)
SRC	92 (1110)	33 (330)	71 (338)	69 (570)	946 (1630)
SRMS	14 (169)	9.1 (91)	16 (76)	8.0 (67)	61(115)
TEC	92 (1110)	63 (630)	67 (319)	27 (220)	277 (477)

TX					
YES1	35 (420)	12 (120)	54 (257)	30 (250)	430 (740)

The data are average of at least two repeated tests. NT: not tested.

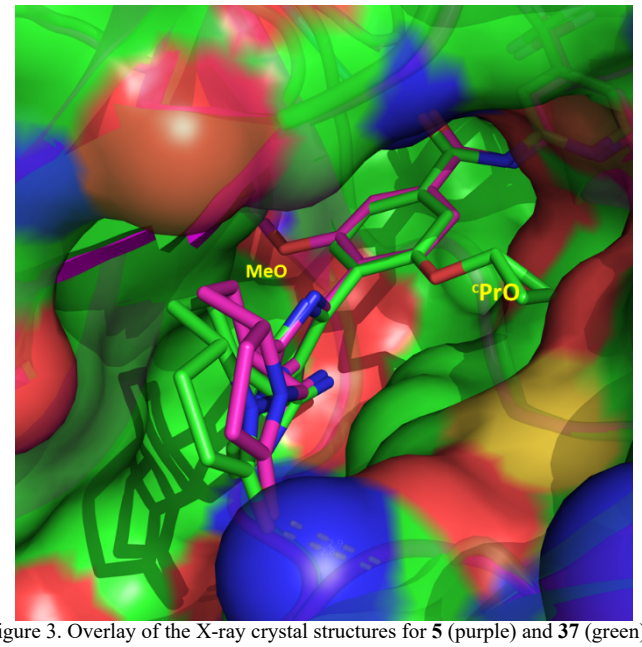

Figure 3. Overlay of the X-ray crystal structures for **5** (purple) and **37** (green), view from the 3-position of the bicyclic ring.

we obtained the X-ray crystal structures[18] for **5** (purple) and **37** (green) bound to BTK enzyme, with overlay shown in Figure 3. The methoxy substitution on **5** and the cyclopropoxy on **37** occupy different pockets of the BTK enzyme. Looking from the bicyclic ring toward the binding pocket, the methoxy on **5** is pointing to the direction of the gate keeper T474 surrounded by a tight hydrophobic pocket, while the cyclopropoxy on **37** is fitting in the opposite side in a relatively bigger pocket. These two pockets of the BTK enzyme allow the substitutions on the phenyl 3-position to provide improved selectivity of BTK over the other kinases tested. But the limited size of these two pockets cannot fit substitutes with size bigger than cyclopropyl.

Several BTK inhibitors of this series were then evaluated in pharmacokinetic tests in preclinical species rats and dogs. The pharmacokinetic parameters for compound **2**, **3**, **4**, **5**, **25** and **37** are listed in Table 5. Compound **3** with the carbamate ring constraint had similar clearance (Cl = 17 ml/min/kg) and half life time (t1/2 = 5.1 h) when dosed IV (2 mg/kg) compared to **2** (Cl = 18 ml/min/kg, t1/2 = 1.8 h).[13] However, **3** had very low oral bioavailability (F = 3.6%), possibly due to the high first pass clearance in liver.

Table 5. Pharmacokinetic parameters of compound **2**, **3**, **4**, **5**, **25** and **37**

Compound	**2**		**3**		**4**		**5**		**25**		**37**	
Rat[a]	IV dose	PO dose	IV dose	PO dose	IV dose	PO dose	IV dose	PO dose	IV dose	PO dose	IV dose	PO dose
Dose (mg/kg)	2	5	2	5	2	5	2	5	2	5	2	5
Cl (mL/min/kg)	18		17		8.0		53		26		42	
Vss (L/kg)	2.6		1.2		0.78		4.0		5.6		4.2	
AUCN (μM*h)	3.1		5.1		7.8		1.1		2.3		1.4	
$T_{1/2}$ (h)	1.8		5.1		2.8		3.0		3.6		2.3	
C_{max} (μM)		0.40		0.34		1.3		0.05		1.0		0.14
T_{max} (h)		1.0		0.25		0.75		2.1		2.5		3.5
F (%)		22		3.6		46		9.5		160		14
Dog[b]	IV dose	PO dose	IV dose	PO dose	IV dose	PO dose	IV dose	PO dose	IV dose	PO dose	IV dose	PO dose
Dose (mg/kg)	1	2			1	2	1	2				
Cl (mL/min/kg)	1.5		NT	NT	11		20		NT	NT	NT	NT
Vss (L/kg)	0.65				1.5		3.0					
AUCN (μM*h)	20				2.8		1.6					
$T_{1/2}$ (h)	6.5				3.6		3.4					
C_{max} (μM)		3.9				1.7		1.1				
T_{max} (h)		2.0				1.0		1.5				
F (%)		82				100		108				

a. Rats for PK test are Wistar Han
b. Dogs for PK test are beagles

To address the high clearance of compound **3**, the gem-dimethyl was introduced on the carbon connected to the carbamate oxygen in compound **25**. A much-improved oral bioavailability (F = 160%) in rats was observed, although the total clearance was still high. The first path clearance by liver was reduced significant for **25**. The lactam constrained compound **4** showed excellent PK profile in both rats and dogs with low clearance, long half-lives and high oral bioavailability. However, when alkoxy substitutions were installed for **5** (MeO) and **37** (cPrO) on the middle phenyl ring, the clearances for both compounds in rats are much higher which lead to low oral exposure. Compound **5** had high clearance and volume distribution in dogs, however, comparable oral exposure in dogs to **4**.

Based on the overall profile of the lead BTK inhibitors listed in Table 5, including potency in enzymatic, cellular and whole blood assays, the kinase selectivities and the PK data, we chose to evaluate compounds **4** and **5** in the rat model of collagen induced arthritis (CIA)[13] for their in vivo efficacy. In a prophylactic treatment protocol, compound **4** demonstrated a dose-dependent

(1, . C.; indicated by significant reduction ($p<0.0001$) of paw thickness through day 30 consequent to CIA induction (Figure 4A). Due to the less optimal PK profile of compound **5** in rats, higher doses (15, 30, 60 and 120 mg/Kg, PO, QD) were required to achieve the similar efficacy in this CIA model with a dose-dependent decrease in the paw thickness (Figure 4B). We were able to demonstrate the in vivo efficacy in the preclinical species with this series of non-covalent reversible BTK inhibitors.

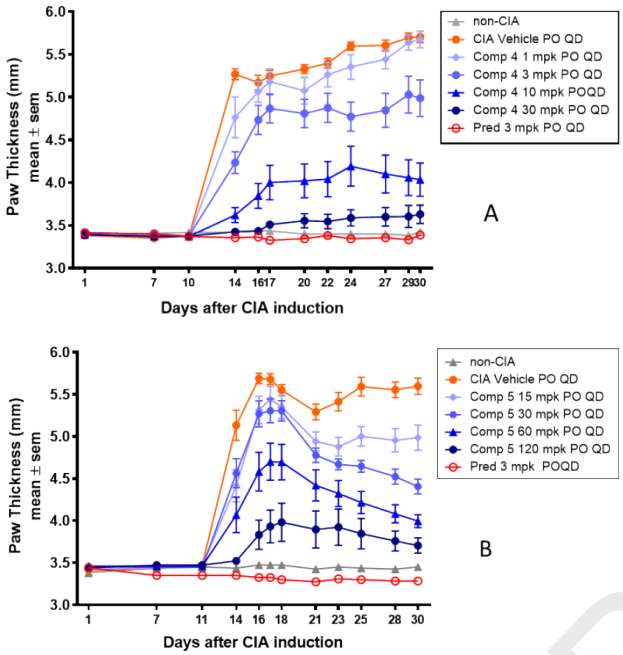

Figure 4. Dose dependent changes in paw thickness in a rat CIA model at different doses of **4** and **5**. Pred = Prednisolone (postive control)

In summary, we described the discovery of a series of non-covalent reversible BTK inhibitors based on the 8-aminoimidazo[1,5-*a*]pyrazine core with various 3-position bicyclic ring substitutes. The cyclic ring constraints lock the carbonyl in the direction to form hydrogen bond with C481 backbone amide NH, which is demonstrated in the X-ray crystal structure of the inhibitor **3** bound to BTK. At the same time, we observed an additional interaction of **3** with N484. Various bicyclic ring substitutes were tolerable to fit into the BTK enzyme binding pockets and maintained potency in the enzymatic, cellular and whole blood assays. Substituents on the middle phenyl 3-position significantly impacted the BTK binding potency and selectivity against the Tec and Src family kinases. This selectivity can be rationalized by the orientation of 3-substituents on **5** and **37** within the pockets around the phenyl ring in the X-ray crystal structures. Compound **4** and **5** have combined desired properties, with potent activities in the BTK enzymatic, cellular, human whole blood assays, the kinase selectivity and *in vivo* pharmacokinetic profile in preclinical species. These orally bioavailable non-covalent reversible BTK inhibitors **4** and **5** displayed dose-dependent efficacy in reducing the paw thickness in the rat collagen induced arthritis model.

References and notes

1. Vetrie, D.; Vorechovsky, I.; Sideras, P.; Holland, J.; Da-vies, A.; Flinter, F.; Hammarstrom, L.; Kinnon, C.; Levinsky, R.; Bobrow, M.; Smith, C. I. E.; Bentley, D. R. *Nature* **1993**, *361*, 226−233.
2. Rhisak, I.; Sparkes, R. S.; Kubagawa, H.; Monafidas, T.; Quan, S.; Belmont, J. W.; Cooper, M. D.; Conley, M. E.; Witte, O. N. **1993**, *72*, 279-290.
3. Kurosaki, T.; Hikida, M. Haslam, *Imm. Rev.* **2009**, *228*, 132-48.
4. Cunningham-Rundles, C.; Ponda, P. P. *Nat. Rev. Immunol.* **2005**, *5*, 880-892.
5. For review: Norman, P. Investigational Bruton's tyrosine kinase inhibitors for the treatment of rheumatoid arthritis *Exp. Opin. Inv. Drugs.* **2019**, *25(8)*, 891-899,.
6. Charalambous, A.; Schwarzbich, M. A.; Witzens-Harig, M. Ibrutinib. In: Martens U. (eds) *Small Molecules in Hematology. Recent Results in Cancer Research*, **2018**, *212*, 242. Springer, Cham.
7. Kriegsmann, K.; Kriegsmann, M.; Witzens-Harig, M. Acalabrutinib, A Second-Generation Bruton's Tyrosine Kinase Inhibitor. In: Martens U. (eds) *Small Molecules in Hematology. Recent Results in Cancer Research*, **2018**, *212*, 285. Springer, Cham.
8. Syed, Y.Y. Zanubrutinib: First Approval. *Drugs* **2020**, *80*, 91–97.
9. Feng, Y.; Duan, W.; Cu, X.; Liang, C.; Min, M. *Exp. Opin. on Thera. Pat.* **2019**, *29 (4)*, 1354-3776.
10. Woyach, J. A.; Furman, R. R.; Liu, T.-M.; Ozer, H. G.; Zapatka, M.; Ruppert, A. S.; Xue, L.; Li, D. H.; Steggerda, S. M.; Versele, M.; Dave, S. S.; Zhang, J.; Yilmaz, A. S.; Jaglowski, S. M.; Blum, K. A.; Lozanski, A.; Lozanski, G.; James, D. F.; Barrientos, J. C.; Lichter, P.; Stilgenbauer, S.; Buggy, J. J.; Chang, B. Y.; Johnson, A. J.; and Byrd, J. C. Resistance Mechanisms for Bruton's Tyrosine Kinase Inhibitor Ibrutinib *The New England J. of Med.*, **2014**, 2286-2294.
11. Crawford, J. J.; Johnson, A. R.; Misner, D. L.; Belmont, L. D.; Castanedo, G.; Choy, R.; Coraggio, M.; Dong, L.; Eigenbrot, C.; Erickson, R.; Ghilardi, N.; Hau, J.; Katewa, A.; Kohli, P. B.; Lee, W.; Joseph W. Lubach, Brent S. McKenzie, Daniel F. Ortwine, Schutt, L.; Tay, S.; Wei, B.; Reif, K.; Liu, L.; Wong, H.; Young, W. B. *J. Med. Chem.* **2018**, *61 (6)*, 2227-2245.
12. Watterson, S. H.; De Lucca, G. V.; Shi, Q.; Langevine, C. M.; Liu, Q.; Batt, D. G.; Bertrand, M. B.; Gong, H.; Dai, J.; Yip, S.; Li, P.; Sun, D.; Wu, D.-R.; Wang, C.; Zhang, Y.; Traeger, S. C.; Pattoli, M. A.; Skala, S.; Cheng, L.; Obermeier, M. T.; Vickery, R.; Discenza, L. N.; D'Arienzo, C. J.; Zhang, Y.; Heimrich, E.; Gillooly, K. M.; Taylor, T. L.; Pulicicchio, C.; McIntyre, K. W.; Galella, M. A.; Tebben, A. J.; Muckelbauer, J. K.; Chang, C.; Rampulla, R.; Mathur, A.; Salter-Cid, L.; Barrish, J. C.; Carter, P. H.; Fura, A.; Burke, J. R.; Tino, J. *J. Med. Chem.* **2016**, *59*, 9173.
13. Liu, J.; Guiadeen, D.; Krikorian, K.; Gao, X.; Wang, J.; Boga, S. B.; Alhassan, A.-B.; Yu, Y.; Vaccaro, H.; Liu, S.; Yang, C.; Wu, H.; Cooper, A.; DeMan, J.; Kaptein, A.; Maloney, K.; Honak, V.; Gao, Y.-G.; Fischmann, T. O.; Raaijmakers, H.; Presland, J.; Mansueto, M.; Xu , Z.; Leccese, E.; Zhang-Hoover, J.; Knemeyer, I.; Garlisi, C. G.; Bays, N.; Stivers, P.; Brandish, P. E.; Hicks, A.; Kim, R.; Kozlowski, J. A. *ACS Med. Chem. Lett.* **2016**, *7 (2)*, 198-203.
14. Gao, X; Wang, J.; Liu, J.; Guiadeen, D.; Krikorian, A.; Boga, S. B.; Alhassan, A.-B.; Selyutin, O.; Yu, W.; Yu, Y.; Anand, R.; Liu,S.; Yang, C.; Wu, H.; Cai, J.; Cooper, A.; Zhu, Hugh; Maloney, K.; Gao, Y.; Fischmann, T. O.; Presland, J.; Mansueto, M.; Xu, Z.; Leccese, E.; Zhang-Hoover, J.; Knemeyer, I.; Garlisi, C. G.; Bays, N.; Stivers, P.; Brandish, P. E.; Hicks, A.; Kim, R.; Kozlowski, J. A. *Bioorg. Med. Chem. Lett.* **2016**, *27*, 1471-1477.
15. Boga, S.B.; Alhassan, A-B.; Liu, J., Guiadeen, D.; Krikorian, A.; Gao, X.; Wang, J.; Yu, Y.; Anand, R.; Liu, S.; Yang, C.; Wu, H.; Cai, J.; Zhu, H.; Desai, J.; Maloney, K.; Gao, Y-D.; Fischmann, T.O.; Presland, J.; Mansueto, M.; Xu, Z.; Leccese, E.; Knemeyer, I.; Garlisi, C.G.; Bays, N.; Stivers, P.; Brandish, P.E.; Hicks, A.; Cooper, A.; Kim, R.M.; Kozlowski, J.A. *Bioorg. Med. Chem. Lett.* **2017**, *27*, 3939-3943.
16. Chang, B. Y.; Huang, M. M.; Francesco, M.; Chen, J.; Sokolove, J.; Magadala, P.; Robinson, W. H.; Buggy, J. J. *Arthritis Res Ther* **2011**, *13*, R115.
17. Detail synthetic experimental procedure can be found at: Kim, R. M.; Liu, J.; Gao, X.; Boga, S. B.; Guiadeen, D.; Kozlowski, J. A.; Yu, W.; Anand, R.; Yu, Y.; Selyutin, O. B.; Gao, Y.; Wu, H.; Liu, S.; Yang, C.; Wang, H. "BTK inhibitors" U.S. Pat. Appl. Publ. **2014**, US 20140206681 A1.
18. The data of X-ray crystal structures for BTK inhibitors **3**, **5** and **37** is up-loaded to the Protein Data Bank (www.pdb.org) with codes 6X3N, 6X3O and 6X3P respectively.